NME1596
pp: 1--22 (col.fig.: nil)
PROD. TYPE: COM
ED: RM
PAGN: Suresh – SCAN: SNagesh

INTERNATIONAL JOURNAL FOR NUMERICAL METHODS IN ENGINEERING
Int. J. Numer. Meth. Engng (in press)
Published online in Wiley InterScience (www.interscience.wiley.com). DOI: 10.1002/nme.1596

Modelling inter-yarn friction in woven fabric armour

X. S. Zeng[‡], V. B. C. Tan[*,†] and V. P. W. Shim[§]

Impact Mechanics Laboratory, Department of Mechanical Engineering, National University of Singapore, 9 Engineering Drive 1, Singapore 117576, Singapore

SUMMARY

The effects of inter-yarn friction on the ballistic performance of woven fabric armour are investigated in this paper. Frictional sliding between yarns is implemented in a computational model of the fabric that takes the form of a network. Yarn crimp and its viscoelastic properties are taken into account. Ballistic experiments are performed to verify the predictions of the model. Parametric studies show that the ballistic response of woven fabric is very sensitive to yarn friction when the friction coefficient is low but insensitive beyond a certain level. The results also show that very high inter-yarn friction can lead to premature yarn rupture, thus reducing the ability of the fabric to absorb impact energy.

KEY WORDS: woven fabric armour; yarn friction; ballistic

1. INTRODUCTION

Advancements in fabric armour have been driven mainly by improvements in the strength and flexibility of the yarns from which they are made. While important, the dynamic response of fabric systems when they are subjected to ballistic impact is not only dependent on the response of individual yarns, but also on the way yarns interact with one another because they are woven together into a fabric system. In addition to materials selection, the design parameters of flexible fabric armour include weave architecture, weave density, surface treatment of the constituent yarns and yarn count—these affect the way yarns interact with one another.

Many studies on the ballistic resistance of fabric systems have been experimental in nature. Ballistic impact tests provide useful information such as relationships between energy absorbed by a fabric and impact energy, high-speed photographic sequences of fabric deformation and post impact analyses of fabric perforation mechanisms. The majority of the experiments are

*Correspondence to: V. B. C. Tan, Impact Mechanics Laboratory, Department of Mechanical Engineering, National University of Singapore, 9 Engineering Drive 1, Singapore 117576, Singapore.
[†]E-mail: mpetanbc@nus.edu.sg
[‡]E-mail: engp2412@nus.edu.sg
[§]E-mail: mpespwv@nus.edu.sg

Received 6 June 2005
Revised 14 September 2005
Accepted 20 October 2005

aimed at identifying the effects of key parameters governing the ballistic performance of a system [1–4].

Computational simulation is increasingly used to investigate the ballistic performance of high-strength fabric as computational cost continues to decrease with the availability of affordable high-performance computing systems. Simulations can yield important information not measurable from experiments when the fabric system is modelled with sufficient detail and accuracy. Many models of woven fabric have been developed. Early models are generally very simplified representations of the woven fabric. For example, Taylor and Vinson [5] treated fabric undergoing ballistic impact as a homogeneous conical shell under quasi-static loading. The model can be considered empirical in that many of the parameters involved require inputs from results of ballistic tests on fabric. Although such membrane models may lack certain details, membrane model representations of woven fabric continue to be used for ballistic impact simulations. Recently, Lim *et al*. [6] studied the ballistic response of fabric using *finite element analysis* by modelling the fabric with isotropic membrane elements. Their emphasis was on developing a constitutive relation to represent the viscoelastic behaviour of the material. Roylance and Wang [7] introduced a more structurally accurate model in the form of a mesh of flexible linear elements pin-jointed at yarn crossover points, where the mass is lumped. Shim *et al*. [8] adopted this fabric model and incorporated yarn crimp and the material viscoelasticity to investigate the ballistic response of cross-woven aramid fabric. The importance of accounting for crimp and dynamic material response was shown through parametric studies and comparison with experimental data.

Recent efforts at simulating the ballistic response of woven fabric have continued in the direction of including more structural features unique to woven fabrics into fabric models and formulating more accurate material models. Johnson *et al*. [9] introduced a FE model using a combination of bar and shell elements. The bar elements modelled the structural response of warp and weft yarns while shell elements provided low-level shear stiffness and grid stability. Many physical parameters like crimp modulus and locking strain were included. Tabiei and Ivanov [10, 11] formulated reduced and fully integrated membrane shell elements for cross-woven fabric and tested the material model using a commercial finite element analysis code (LS-DYNA). The material model was derived by a homogenization technique to describe fabric micro-mechanical models via an effective stiffness matrix. The material model took into account certain special characteristics of a fabric, such as reorientation and locking of yarns during impact. Shockey *et al*. [12] created finite element models of individual yarns using 3-dimensional brick elements and assembled them to form a woven fabric. Each yarn was discretized into eight hexahedral elements over its cross section and 12 elements along a crimp wavelength. While the model could include many details of the woven architecture, it also increased the computation time significantly because of the large number of degrees of freedom (DOF). Duan *et al*. [13, 14] presented a similar FE model in LS-DYNA, which was able to account for yarn sliding and frictional effects between interwoven yarns. Their parametric study showed that friction between yarns facilitates energy dissipation within the fabric target.

While it is now possible to perform computational simulations of ballistic impact on fabric systems using models where the yarns are fully discretized into fine solid finite elements, such models still remain computationally expensive. The focus of this paper is to implement sliding between yarns in the fabric models presented by Roylance and Wang [7] and Shim *et al*. [8] while maintaining computational efficiency. Yarn–yarn interactions at crossover

points are responsible for transmitting energy from yarns in contact with the projectile (primary yarns) to yarns that are not (secondary yarns) [15]. The interactions also affect the way the fabric is perforated by the projectiles. Various effects of yarn–yarn friction have been reported. Prosser [16] analysed fabrics impacted by 0.22 calibre fragment simulating projectiles (FSP) and found that if slippage could be reduced by just four yarns at the impact point, an almost 50% increase in protection could be achieved. Bazhenov [17] reported that in multiple-ply fabric systems, the ravelling of yarns at the unclamped edges is related to the energy transferred to yarns in each fabric layer. It is believed that yarn slippage generated additional energy dissipation via friction associated with slippage at crossover points. Impact experiments [1, 2, 18] have been designed to investigate the effects of yarn friction on fabric ballistic resistance by using chemical treatment to vary the yarn surface roughness. It was found that fabrics with a high friction coefficient dissipated larger amounts of energy. Lee *et al*. [19] performed static penetration tests on dry fabric and on a low resin content fabric-reinforced composite and showed that the composite can absorb more energy than the dry fabric specimen because yarn sliding is reduced.

In this paper, the interwoven yarn structure of fabrics is physically modelled to allow for yarn slippage between yarns with friction. Fabric models which take yarn slippage into account are currently limited to FE models where the yarns are fully discretized into solid elements such as those of Shockey *et al*. [12] and Duan *et al*. [14]. The proposed model is able to include yarn slippage using significantly smaller number of degrees of freedom.

2. NUMERICAL MODEL OF WOVEN FABRIC

The plain weave is one of the most common weave patterns for armour-grade fabric. Each yarn in the warp direction passes alternately under and over an orthogonal yarn in the weft direction. In the proposed fabric model, each yarn in the fabric is modelled by a zigzag chain of linear elements pin-jointed together at nodal points. Each node is assigned a lumped mass to represent the areal density of the fabric. Figure 1 shows the fabric model before it is impacted by the projectile. Initially, the nodes coincide with yarn crossover points. For a balanced plain-woven fabric, the geometry of the fabric model is completely described by two parameters—the distance L_0 between neighbouring nodes on a yarn and the distance L_1 between a pair of nodes at a crossover point. L_1 can be determined by the fabric thickness and L_0 can be determined by the number of yarns per unit length along warp/weft direction. These parameters are normally available from the fabric specifications or are easily measured.

The explicit computational simulation proceeds at incremental time steps and is adopted from the work of Shim *et al*. [8]. Nodal positions and velocities are updated after each time step increment using a central time difference integration scheme. The nodal velocity at time $t + \Delta t$ is computed from,

$$\mathbf{v}_{t+\Delta t} = \mathbf{v}_t + \frac{\Delta t}{m} \sum \mathbf{f} \tag{1}$$

where $\sum \mathbf{f}$ is the resultant force acting on the node arising from tension in the two connected yarn elements, and m is the mass of the node. The nodal position is then updated using

$$\mathbf{x}_{t+\Delta t} = \mathbf{x}_t + \mathbf{v}_{t+\Delta t} \Delta t \tag{2}$$

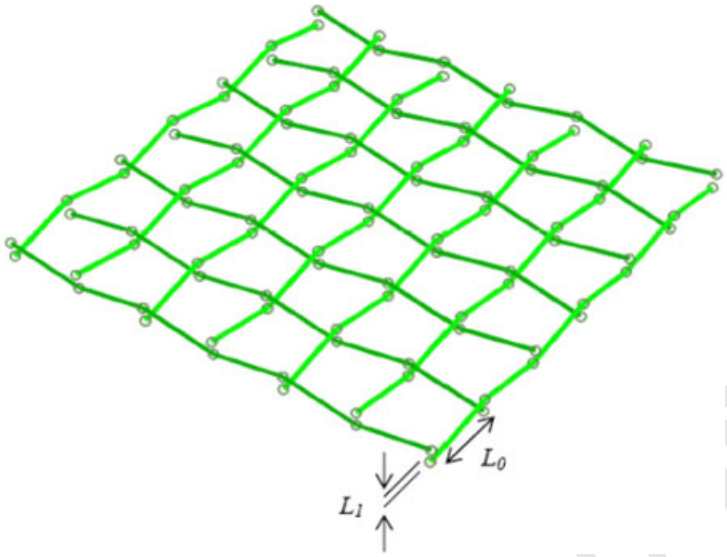

Color Online, B&W in Print

Figure 1. Network model for cross-woven fabric.

The force $\mathbf{f}$ is computed via a viscoelastic constitutive equation, written generically as

$$\mathbf{f}_{t+\Delta t} = \varphi(\boldsymbol{\sigma}_t, \boldsymbol{\varepsilon}_t, \boldsymbol{\varepsilon}_{t+\Delta t}) \tag{3}$$

where the stress, $\boldsymbol{\sigma}$, and strain, $\boldsymbol{\varepsilon}$, are calculated for each linear yarn element.

Equations (1)–(3) are applied to all the nodes first without consideration of possible interpenetration of nodes into the surface of the projectile or interpenetration of yarn elements. The nodal co-ordinates and velocities are then adjusted to exclude interpenetration in the subsequent step through two contact algorithms—one for yarn-to-yarn contact and another for fabric-to-projectile contact.

3. ALGORITHM FOR CONTACT BETWEEN YARN ELEMENTS

At each time step, a check is made to determine if any yarn element has interpenetrated another element. Instead of implementing a general contact algorithm, it was observed from post-impact specimens of cross-woven fabric that a simplified contact algorithm tailored for yarn-to-yarn contact would suffice because,

- any pair of warp and weft yarns are in contact with each other at no more than one location, except for the case of ravelled yarns along the fabric edges, and
- weft yarns are prevented from contacting adjacent weft yarns by the interwoven warp yarns and *vice versa* because armour-grade fabrics are tightly woven.

After the nodal positions are updated by Equation (2), the nearest points between each pair of warp and weft yarns are determined. Their relative position will dictate if interpenetration has occurred. The nearest nodes between each warp and weft pair are first identified. A small

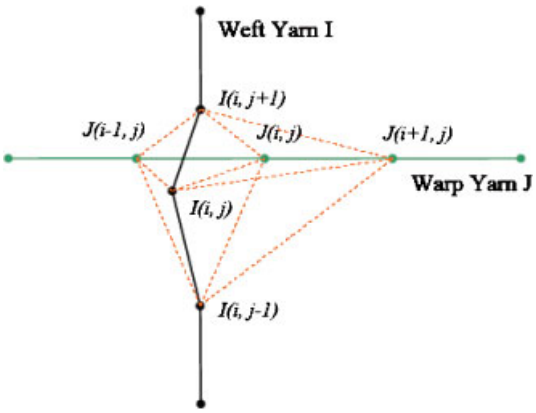

Color Online, B&W in Print

Figure 2. Orthogonal yarn elements (dashed lines indicate probable pairs of nearest nodes).

time step size for the explicit computation means that the configuration of the fabric model changes only incrementally between time steps. The maximum time step increment Δt required for numerical stability is described by Shim *et al.* [8]—Δt must be smaller than the time for stress wave to propagate through one single linear element, i.e.

$$\Delta t \leqslant \alpha \frac{L}{c} \tag{4}$$

where L is the length of one linear segment in the model, $c = \sqrt{E/\rho}$ (the wave speed in a single yarn) and α a positive constant less than unity.

The use of a small time step means that the nearest pair of nodes can change by at most only one node along the yarns between time steps. Hence, if nodes $I(i, j)$ and $J(i, j)$ in Figure 2 are the nearest pair in the previous time step for weft yarn I and warp yarn J, it is sufficient to compare the distances between nodes $I(i, j-1)$, $I(i, j)$, $I(i, j+1)$ and nodes $J(i-1, j)$, $J(i, j)$, $J(i+1, j)$ to determine the nearest nodes for the current time step.

Assuming nodes $I(i, j)$ and $J(i, j)$ are the closest pair of nodes, as shown in Figure 3, then the point on yarn I closest to yarn J is assumed to lie between nodes $I(i, j-1)$ and $I(i, j+1)$. Similarly, the point on yarn J closest to yarn I is assumed to lie between nodes $J(i-1, j)$ and $J(i+1, j)$. The four yarn segments in Figure 3 are denoted by vectors $\mathbf{i}_\alpha$ and $\mathbf{j}_\beta$ $(\alpha, \beta = 1, 2)$ as shown. The relative position of a point on a yarn segment of yarn J from a point on a yarn segment of yarn I is given by

$$\mathbf{d} = \overrightarrow{IJ} - a\mathbf{i}_\alpha + b\mathbf{j}_\beta \tag{5}$$

where $\overrightarrow{IJ}$ is the vector from node $I(i, j)$ to node $J(i, j)$ and $(0 \leqslant a, b \leqslant 1)$.

The shortest distance between the two yarns is given by the minima of $|\mathbf{d}|$ with respect to a and b, i.e.

$$\begin{bmatrix} \partial|\mathbf{d}|/\partial a \\ \partial|\mathbf{d}|/\partial b \end{bmatrix} = \mathbf{0} \tag{6}$$

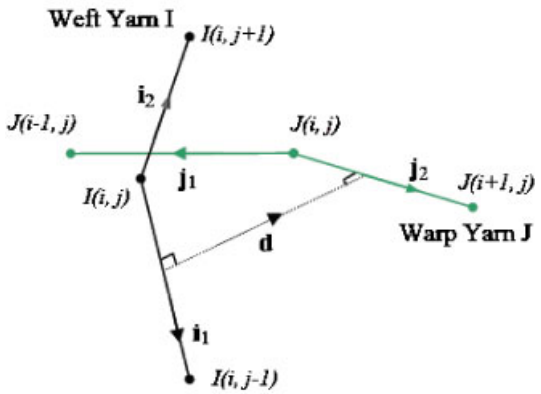

Color Online, B&W in Print

Figure 3. Definition of contact vector (**d**) and yarn vectors (**i**, **j**) for nearest node pair $I(i, j)$ and $J(i, j)$.

Combining Equations (5) and (6) gives

$$\begin{bmatrix} -\mathbf{i}_\alpha \cdot (\overrightarrow{IJ} - a\mathbf{i}_\alpha + b\mathbf{j}_\beta) \\ \mathbf{j}_\beta \cdot (\overrightarrow{IJ} - a\mathbf{i}_\alpha + b\mathbf{j}_\beta) \end{bmatrix} = \mathbf{0} \tag{7}$$

Equation (7) can be expressed as

$$\begin{bmatrix} \mathbf{i}_\alpha \cdot \mathbf{i}_\alpha & -\mathbf{i}_\alpha \cdot \mathbf{j}_\beta \\ -\mathbf{i}_\alpha \cdot \mathbf{j}_\beta & \mathbf{j}_\beta \cdot \mathbf{j}_\beta \end{bmatrix} \begin{bmatrix} a \\ b \end{bmatrix} = \begin{bmatrix} \overrightarrow{IJ} \cdot \mathbf{i}_\alpha \\ \overrightarrow{JI} \cdot \mathbf{j}_\beta \end{bmatrix} \tag{8}$$

Equation (8) is solved for a and b to locate the points on the two yarn segments closest to each other after which, **d** can be determined from (5). The pair of yarn segments with the lowest value of $|\mathbf{d}|$ is then checked for interpenetration. It should be noted that **d** is normal to a plane parallel to $\mathbf{i}_\alpha$ and $\mathbf{j}_\beta$ and is referred to as the contact vector.

Figure 4 shows a warp yarn, I, going over and under adjacent weft yarns, J and $J+1$. Node numbers along all warp yarns increase from bottom to top and node numbers along weft yarns increase from left to right. For every warp yarn element, $\mathbf{i}^+$ is a vector along the yarn element in the direction of increasing node number. A vector $\mathbf{j}^+$ is similarly defined for weft yarn elements. It can be seen from Figure 4 that a vector pointing from yarn I to yarn J at their crossover point is given by $\mathbf{n} = -\mathbf{i}^+ \times \mathbf{j}^+$, where $\mathbf{i}^+$ and $\mathbf{j}^+$ are associated with the yarn segments in contact. The crossover point may change as yarns I and J slide along one another, however, $-\mathbf{i}^+ \times \mathbf{j}^+$ will continue to indicate the relative position of yarn J with respect to I. Hence, if contact vector **d** points in the opposite direction to **n**, it indicates that interpenetration has occurred. Interpenetration of other weft–warp yarn pairs is detected in the same manner. It should be noted that for some pairs of weft and warp yarns, the vector pointing from the warp to the weft yarn is given by $\mathbf{n} = \mathbf{i}^+ \times \mathbf{j}^+$ instead, as is the case for yarns I and $J+1$. The vector **n** is determined for each pair of weft and warp yarn based on the weave pattern of the fabric prior to the start of the computation. Each yarn segment is considered to be a cylindrical

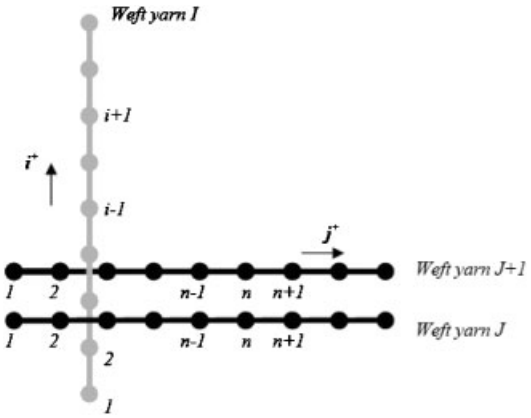

Figure 4. Node numbering for weft and warp yarns and definition of vectors $\mathbf{i}^+$ and $\mathbf{j}^+$.

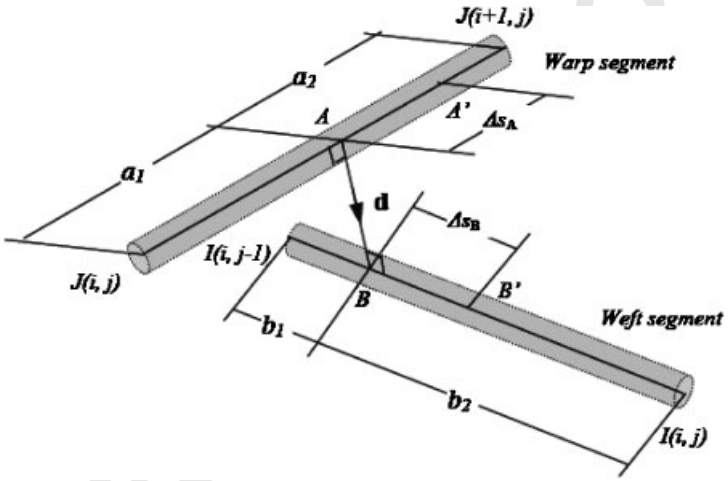

Figure 5. Illustration of interpenetrating yarn segments showing previous points of contact, A' and B'.

rod with a diameter D equivalent to half of the fabric thickness, hence, interpenetration also occurs if $|\mathbf{d}|$ is smaller than D.

The usual master-slave contact method to correct for interpenetration is not imposed here because inter-yarn contact is symmetric. Instead, an adjustment is made to the nodal velocities of interpenetrating yarn segments to move the yarn segments back toward the surface of each other within a single time step. Figure 5 shows two interpenetrating segments before any correction is made. Points A and B are the closest points on the segments and the magnitude of the interpenetration is $\delta = |\mathbf{d}| + D$. Hence, an adjustment of δ along vector $\mathbf{d}$ is to be made to the relative position of the yarn segments. Point A divides the warp yarn segment in the ratio of $a_1 : a_2$, $(a_1 + a_2 = 1)$ and point B divides the weft yarn segment in the ratio of $b_1 : b_2$,

$(b_1 + b_2 = 1)$. To move the segments by a total of δ, the velocity of the nodes connected to the contacting segments are adjusted by

$$\begin{aligned} \Delta\mathbf{v}_{J(i,j)} &= -a_2\Delta\mathbf{v} \qquad & \Delta\mathbf{v}_{I(i,j-1)} &= b_2\Delta\mathbf{v} \\ \Delta\mathbf{v}_{J(i+1,j)} &= -a_1\Delta\mathbf{v} \qquad \text{and} & \Delta\mathbf{v}_{I(i,j)} &= b_1\Delta\mathbf{v} \end{aligned} \tag{9}$$

where

$$|\Delta\mathbf{v}| = -\frac{\delta}{\Delta t(a_1^2 + a_2^2 + b_1^2 + b_2^2)} \tag{10}$$

and Δt is the time step increment for computation.

The velocity adjustments will result in a relative displacement of δ within a time step and the total linear and angular momentum of the yarn segments before and after the velocity correction are conserved. The end result is similar to a normal contact force $\mathbf{f}_n$ pushing points A and B back toward their yarn surfaces, where

$$\mathbf{f}_n = m\frac{\Delta\mathbf{v}}{\Delta\mathbf{t}} \tag{11}$$

After adjustments to the nodal velocities to correct for yarn interpenetration as described, further adjustments are made to account for frictional forces due to sliding of yarn elements over one another during contact. The treatment of contact between rod elements formulated by Zavarise and Wriggers [20] is adopted and modified for the current finite difference implementation.

A' and B' in Figure 5 represent the points of contact between the two segments in the previous time step. This means that the warp yarn J has slid along yarn I by a distance of Δs_A within a time interval of Δt.

A trial friction force is first computed by a penalty formulation

$$\mathbf{f}_t^{\text{trial}} = K\Delta\mathbf{s}_A \tag{12}$$

K is a penalty parameter defined by $K = \alpha(m/\Delta t^2)$, where m is the nodal mass and α is a factor $\alpha \leqslant 1.0$. The trial friction force is applied to yarn J in the direction $\overrightarrow{A'A}$. When $\alpha = 1$, $\mathbf{f}_t^{\text{trial}}$ is equivalent to the force required to move the yarn segments back to the contact configuration in the previous time step.

A frictional slippage function based on Coulomb friction is used to determine if sliding occurs. The magnitude of the trial friction force is compared to the maximum Coulombic friction force, i.e.

$$\varphi = |\mathbf{f}_t^{\text{trial}}| - \mu|\mathbf{f}_n| \tag{13}$$

where μ is the friction coefficient and $\mathbf{f}_n$ is obtained from Equation (11). If φ is negative, no slippage occurs. The force applied to the J yarn element is $\mathbf{f}_t = \mathbf{f}_t^{\text{trial}}$ in the direction $\overrightarrow{A'A}$ and the point A' is recorded as the point of contact on yarn J. A positive value of φ indicates slippage. In this case, the force applied to the J yarn element is $\mathbf{f}_t = \mu\mathbf{f}_n$ and the new contact position on yarn J relative to A' is

$$\Delta s_A = \frac{|\mathbf{f}_t^{\text{trial}}| - \mu|\mathbf{f}_n|}{K} \tag{14}$$

Figure 5 also shows that the point of contact on yarn I moving from B' to B in the absence of friction. When friction is present, the frictional force to be applied to yarn I is determined in the same manner as for yarn J. It should be noted that the friction force $\mathbf{f}_t$ applied to yarn J will also be applied to yarn I but in the opposite direction and *vice versa*, i.e. the actual friction force $\mathbf{f}_f$ acting at the contact point is the resultant of the two tangential forces along the beam axes. The velocity changes for each node arising from friction can be calculated from

$$\Delta\mathbf{v}_{J(i,j)} = -a_2 \frac{\mathbf{f}_f \Delta t}{m} \qquad \Delta\mathbf{v}_{I(i,j-1)} = b_2 \frac{\mathbf{f}_f \Delta t}{m}$$
$$\text{and} \tag{15}$$
$$\Delta\mathbf{v}_{J(i+1,j)} = -a_1 \frac{\mathbf{f}_f \Delta t}{m} \qquad \Delta\mathbf{v}_{I(i,j)} = b_1 \frac{\mathbf{f}_f \Delta t}{m}$$

Although the flexural rigidity of yarns is minimal, a small amount of bending stiffness between interconnecting yarn segments is necessary to prevent unrestricted rotation of the pin-jointed yarn elements. For this purpose, a compressive 'spring' equivalent to 5% the stiffness of the yarn elements connects the middle of adjoining yarn elements.

It is possible to improve the accuracy of the yarn-to-yarn contact algorithm by performing multiple iterations of the procedures described to Equations (5)–(15) in a single time step. Johnson and Stryk [21] introduced this technique to obtain better compatibility between the surfaces of master and slave elements for contact and sliding interface problems. Within one time step, N iterations were carried out to gradually correct surface interpenetration and include sliding frictional forces. A fraction, α, of the required position and velocity changes is made within one iteration, where α is determined from

$$\alpha = \frac{1}{\sqrt{N-n-1}} \tag{16}$$

where N is the specified total number of iterations and n is the current iteration number. Within each iteration, the algorithm updates the contact information after making fine adjustments to the nodal positions. For this iterative procedure Equation (10) is modified to

$$|\Delta\mathbf{v}| = -\alpha \frac{\delta}{\Delta t\,(a_1^2 + a_2^2 + b_1^2 + b_2^2)} \tag{17}$$

4. ALGORITHM FOR SLIDING CONTACT WITH FRICTION BETWEEN FABRIC AND PROJECTILE

In the computational simulation, the projectile is modelled as a rigid sphere striking a rectangular fabric target normally at the centre. Hence, only a quarter of the fabric needs to be modelled because of the double symmetry, and rotation of the projectile need not be considered.

The effect of friction between yarn elements and the projectile is accounted for in the simulation. As with yarn-to-yarn interactions, the position of the projectile and the fabric nodes are initially updated without considering contact between the projectile and fabric. After the initial position update, some fabric nodes may have interpenetrated the projectile surface.

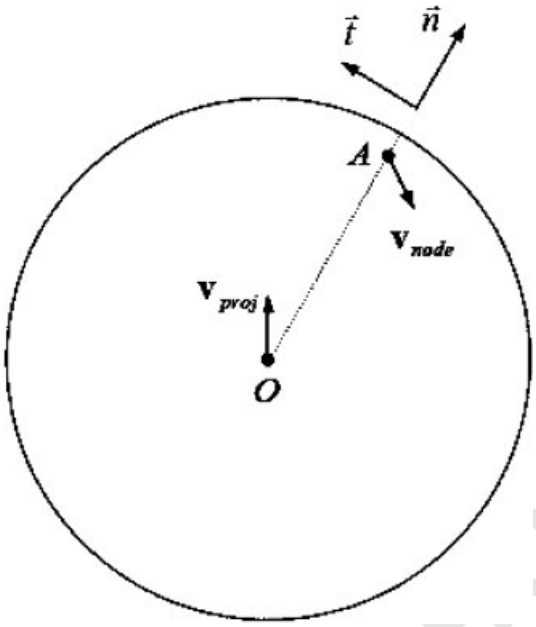

Figure 6. Interpenetration of yarn node A into spherical projectile.

Interpenetration occurs when

$$D_{\text{node}} = |\mathbf{x}_{\text{node}} - \mathbf{x}_{\text{proj}}| \leqslant R_{\text{proj}} \tag{18}$$

Here, R_{proj} is the radius of the projectile, $\mathbf{x}_{\text{node}}$ is the position vector of the node and $\mathbf{x}_{\text{proj}}$ is the position vector of the projectile centre O. Figure 6 shows the situation where a node, A, has interpenetrated the projectile. Node A is treated as a slave node and a force, $\mathbf{f}_{\text{n}}^{p}$, normal to the projectile surface (i.e. in the radial direction $\mathbf{n}$, of the spherical projectile) is applied to the node to push it back onto the projectile surface within one time step. This force is determined from

$$\mathbf{f}_{\text{n}}^{p} = \frac{m(R_{\text{proj}} - D_{\text{node}})}{\Delta t^2}\,\mathbf{n} \tag{19}$$

In the presence of friction, the frictional force acting on the node, $\mathbf{f}_{\text{t}}^{p}$, also needs to be found. The relative velocity of the node to the projectile is first determined, i.e.

$$\mathbf{v}_{\text{R}} = \mathbf{v}_{\text{node}} - \mathbf{v}_{\text{proj}} \tag{20}$$

The component of $\mathbf{v}_{\text{R}}$ normal to $\mathbf{n}$ determines the direction of the frictional force and is given by

$$\mathbf{v}_{\text{R}}^{t} = \mathbf{v}_{\text{R}} - (\mathbf{v}_{\text{R}} \cdot \mathbf{n})\mathbf{n} \tag{21}$$

The tangential force applied to the node is then

$$\mathbf{f}_{\mathrm{t}}^{p} = -\min\left(m\frac{\mathbf{v}_{\mathrm{R}}^{t}}{\Delta t}, \mu_P|\mathbf{f}_P^n|\mathbf{t}\right) \tag{22}$$

where μ_P is the Coulomb friction coefficient between the fabric and projectile and $\mathbf{t}$ is the unit vector parallel to $\mathbf{v}_{\mathrm{R}}^{t}$.

5. COMPUTATIONAL SIMULATION OF WOVEN ARAMID FABRIC

Actual ballistic tests were performed by launching 12 mm (7 g) spherical steel projectiles to strike 120×120 mm Twaron® CT 716 fabric specimens clamped along two opposite edges, with normal incidence. Twaron® is made from aramid (PPTA) fibrous material, similar to that of Kevlar®. The algorithms described were implemented to simulate the ballistic experiments and the relevant specifications of the fabric are listed in Table I. From the specifications, the parameters to construct the woven fabric network structure shown in Figure 1 were ascertained to be $L_1 = 0.2$ mm and $L_0 = 0.844$ mm, and the nodal mass was calculated to assume the value $m = 9.4 \times 10^{-5}$ g.

The material constitutive relationship for yarn elements in the fabric model is represented by a linear spring–dashpot Zener viscoelastic model to describe the strain rate sensitivity of the polymer fibre [6]. The constitutive relationship is described by

$$\left(1 + \frac{K_2}{K_1}\right)\sigma + \frac{\mu_2}{K_1}\dot{\sigma} = K_2\varepsilon + \mu_2\dot{\varepsilon} \tag{23}$$

where σ, ε and $\dot{\varepsilon}$ are the stress, strain and strain rate, respectively. The constants defining the springs (K_1, K_2) and dashpot (μ) are obtained semi-empirically. At a constant strain rate, i.e. $\dot{\varepsilon}(t) = \mathrm{d}\varepsilon(t)/\mathrm{d}t = \dot{\varepsilon}_0$, the stress as a function of strain and strain rate, with initial conditions $\varepsilon = 0$ and $\sigma = 0$, corresponding to Equation (23) are

$$\sigma = \frac{K_1K_2}{K_1 + K_2}\varepsilon - \frac{K_1^2\mu}{(K_1 + K_2)^2}\dot{\varepsilon}_0(\mathrm{e}^{-((K_1+K_2)/\mu)\varepsilon/\dot{\varepsilon}_0} - 1) \tag{24}$$

and

$$\frac{\mathrm{d}\sigma}{\mathrm{d}\varepsilon} = \frac{K_1K_2}{K_1 + K_2} + \frac{K_1^2}{K_1 + K_2}(\mathrm{e}^{-((K_1+K_2)/\mu)\varepsilon/\dot{\varepsilon}_0}) \tag{25}$$

Experimental data for Twaron yarns at different strain rates is scarce. Here, use of data reported by Gu [22] as shown in Table II, is employed. The values of the parameters for the viscoelastic material model are obtained from the best fit of Equation (25) to the reported Young's modulus, as shown in Figure 7. These values are $K_1 = 7.28 \times 10^{10}$ Pa, $K_2 = 4.17 \times 10^{11}$ Pa and $\mu = 6.26 \times 10^{8}$ Pa s. The failure strain of yarn elements is approximated to be within the range of 5.2–5.7%.

The numerical model is implemented through an in-house code and simulations are performed on a 2.8 GHz Pentium IV personal computer. The time taken to complete a simulation depends on the assigned impact velocity of the projectile. For low impact velocities, the penetration

Table I. Twaron® fabric CT716 specification.

Specific density	1.44 g/cm^3
Linear density warp and weft	1100 dtex f 1000
Areal density	280 g/m^2
Thickness	0.40 mm
Sett (per 10 cm)	122

Table II. Twaron® fibre bundle properties [22].

Strain rate (s^{-1})	E(GPa)	ε_{max} (%)
10^{-2}	62	5.19
180	69	5.22
480	70	5.47
1000	72	5.70

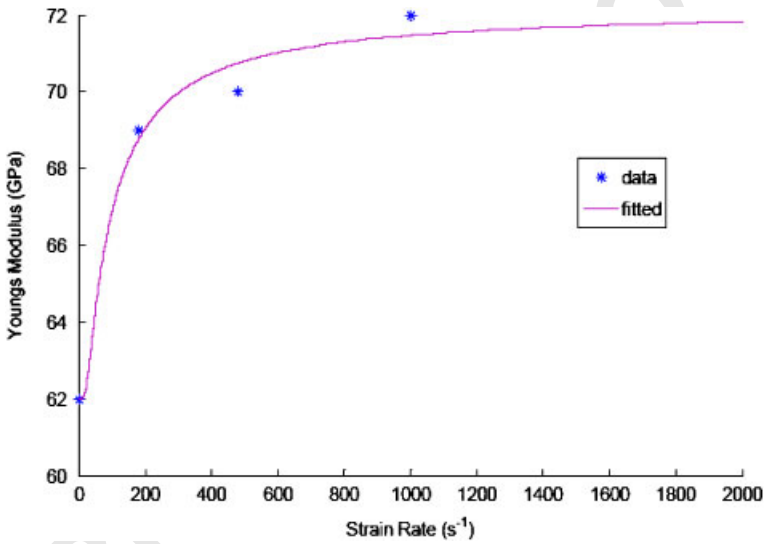

Color Online, B&W in Print

Figure 7. Variation of Young's modulus with strain rate based on Equation (24) and fit with experimental data from Gu [22].

process is slow and the simulations take about 1–2 h of computational time whereas high-velocity impacts require only a few minutes.

6. VALIDATION OF FABRIC MODEL

The effects of yarn-to-yarn friction were investigated in this paper by performing simulations over a range of friction coefficients. Briscoe and Motamedi [18] measured the friction coefficient

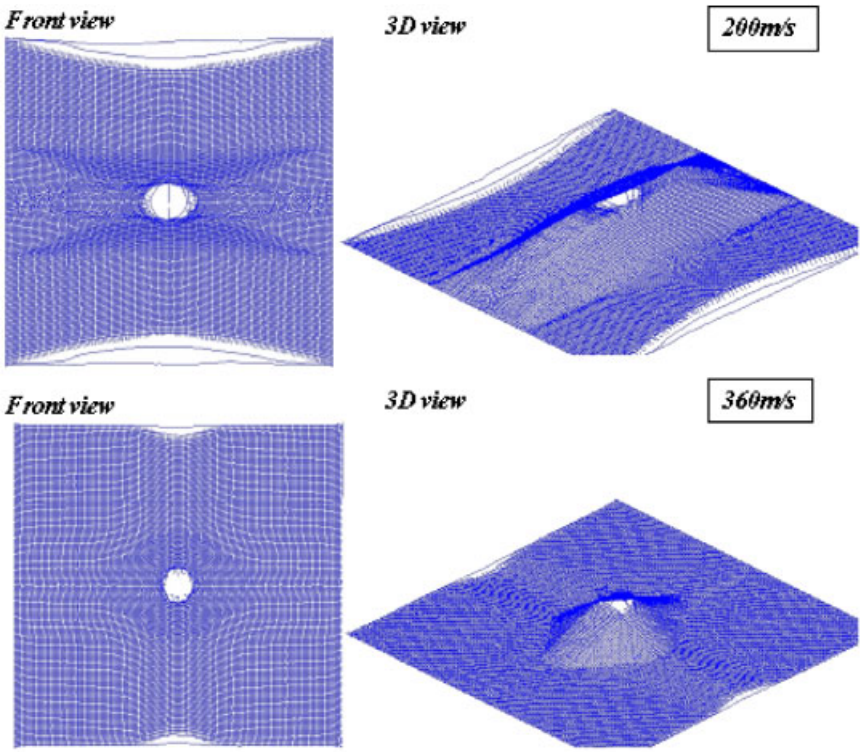

Color Online, B&W in Print

Figure 8. Predicted fabric perforation characteristics for impact at 200 and 360 m/s.

of the aramid yarn, Kevlar® 49, by using a hanging-yarn experimental method and reported values of $\mu = 0.22 \pm 0.03$. Rebouillat [23] studied the effects of relative sliding speed on the friction coefficient between Kevlar® yarns using a classical pin-on-disc tribometer. The yarn coefficient of friction was reported to be $\mu = 0.22 \pm 0.03$ at a sliding speed of 9.6 mm/min and $\mu = 0.27 \pm 0.03$ at a speed of 77×10^3 mm/min.

Figure 8 shows the deformation predicted by the fabric model with $\mu = 0.2$, after perforation by a projectile striking at 200 and 360 m/s, respectively. The configurations predicted by the computational model correlate closely with experimental observations. Deformation at low impact velocity differs from that at high impact velocity. For an impact velocity of 200 m/s, the fabric was fully stretched prior to perforation and a large area of fabric was deflected. At 360 m/s, the transverse waves did not have enough time to propagate to the edges before the perforation occurred, resulting in a small area of deflection. Similar observations have been captured by high-speed photographs of ballistic tests, as shown in Figure 9.

The simulations also identified differences in the way the yarns break at the region of impact, as shown in Figure 8. At a relatively low velocity of 200 m/s, the number of broken warp and weft yarns differs significantly. Clamped yarns broke earlier than unclamped yarns because unclamped yarns do not elongate significantly during impact. As the fabric deflects, the unclamped yarns are simply pulled inwards whereas clamped yarns need to stretch to

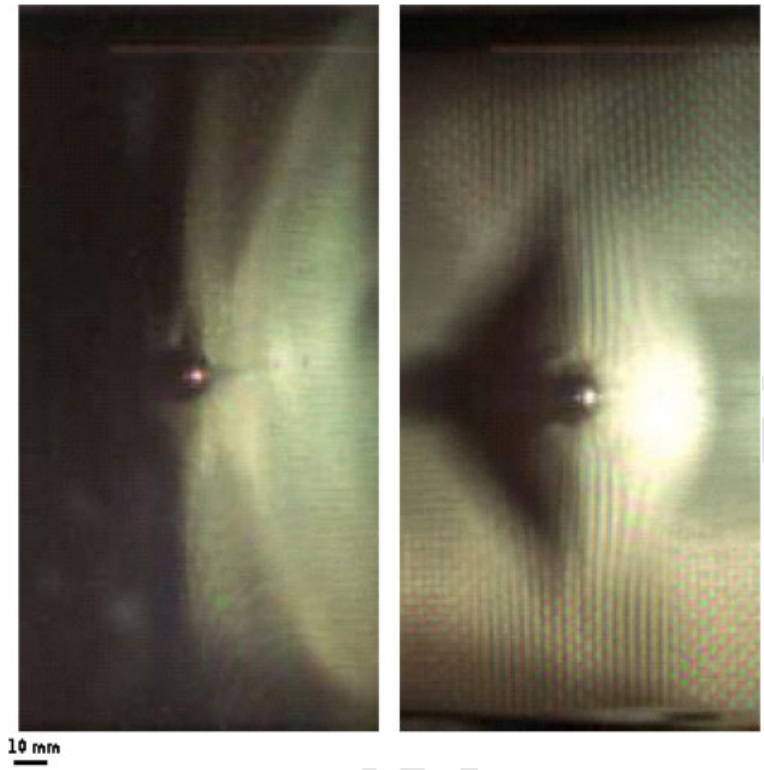

Color Online, B&W in Print

Figure 9. High-speed photographs of fabric perforation; left: low-velocity impact 200 m/s; right: high-velocity impact 360 m/s.

accommodate the fabric deflection. As a consequence, the primary clamped yarns rupture to form a slit, while most of the unclamped yarns are able to slide against the projectile without breaking. Only a few unclamped yarns remain in contact with the projectile and are pulled to breakage. At a high impact velocity like 400 m/s, the fabric is perforated within a very short time. Boundary conditions have less influence at high impact velocities because the fabric is perforated before the primary yarns are uniformly stretched. Hence, the numbers of yarns broken in the weft and warp directions are almost equal giving rise to square rather than slit-like perforations. These features are also observed in actual fabric specimens, as illustrated in Figure 10.

Another physical phenomenon that was replicated in the simulation is the ravelling of yarns along the free edges. This ravelling gives an indication of the amount of energy that is transmitted to the edges of the fabric.

The energy absorbed by a fabric during impact is one measure of its ballistic resistance to small projectiles. As indicated in Table II, the failure strain varies with strain rate [22]. Computational simulations were performed using failure strains at the lower and upper bounds of 5.2 and 5.7% for comparison. Simulation results of energy absorbed by the fabric over an impact velocity range of 180–500 m/s are plotted together with experimental data in Figure 11.

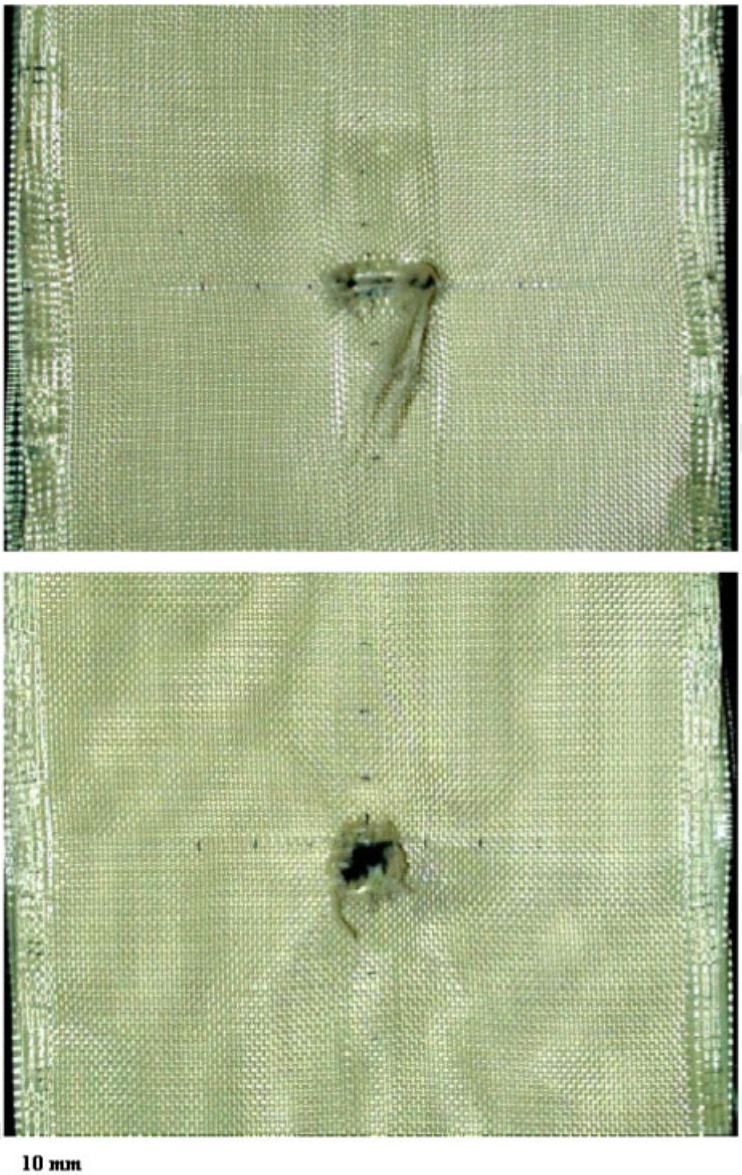

Color Online, B&W in Print

Figure 10. Single fabric ply after penetration, left: low-velocity impact 200 m/s, right: high-velocity impact 360 m/s.

The graphs show reasonable agreement between simulation and experiments. Both numerical and simulation results display a sudden decrease in energy absorption at about 250 m/s. It should be noted that the material properties were based on experimental results from Gu [22] and not from tests on the Twaron® fabric used in the ballistic tests reported. Hence, only qualitative

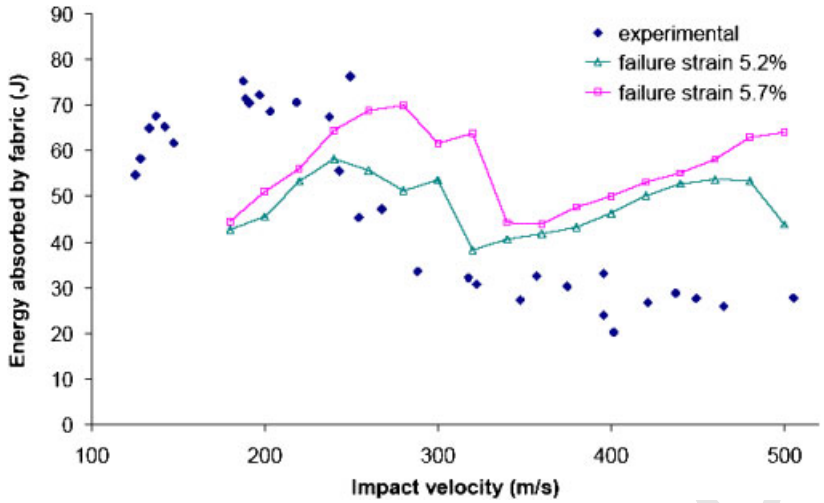

Color Online, B&W in Print

Figure 11. Variation of energy absorbed by fabric with impact velocity—simulation and ballistic test results.

comparisons are possible. Quantitative comparisons will require actual material properties of the yarns from the fabric tested. A comparison of ballistic tests results for Twaron® fabric with simulation using yarn properties from Gu [22] verifies that the mechanisms of fabric deformation and perforation are reflected by the model and that predicted trends in energy absorption are similar to experimental results.

7. EFFECTS OF FRICTION COEFFICIENT ON ENERGY ABSORBED BY FABRIC

A parametric study on the effects of friction coefficient was carried out by varying the coefficient of friction between yarns from 0 to 1. The friction coefficient between the projectile and the yarn is kept constant as 0.27 as measured in Reference [23] for all simulations. Different yarn–yarn friction coefficients resulted in differences in the penetration processes, as shown in Figure 12. A low friction ($\mu = 0.02$) corresponds to a fabric with very low structural coherence. It allows a projectile to push yarns aside easily and adversely affects the ability of the fabric to retard the projectile. For a more realistic friction level ($\mu = 0.2$), the numerical model predicts fabric perforation that correlates closely with experimental observations. It also shows that unclamped yarns are less likely to rupture than clamped yarns. A high contact friction ($\mu = 1.0$) reduces yarn mobility and inter-yarn sliding. Hence, yarns in both unclamped and clamped directions break at the same time.

The trends of energy absorption by fabric for different yarn friction coefficients are presented in Figure 13. The range of coefficient is categorized into three groups—low ($\mu = 0$–0.06), moderate ($\mu = 0.06$–0.2) and high ($\mu = 0.2$–1)—based on their effects on energy absorption by the fabric. For a low friction coefficient, the energy absorbed by the fabric increases with impact velocity as well as with the friction coefficient. Energy absorption is strongly sensitive to the magnitude of friction coefficient within this range of coefficients. For moderate coefficients

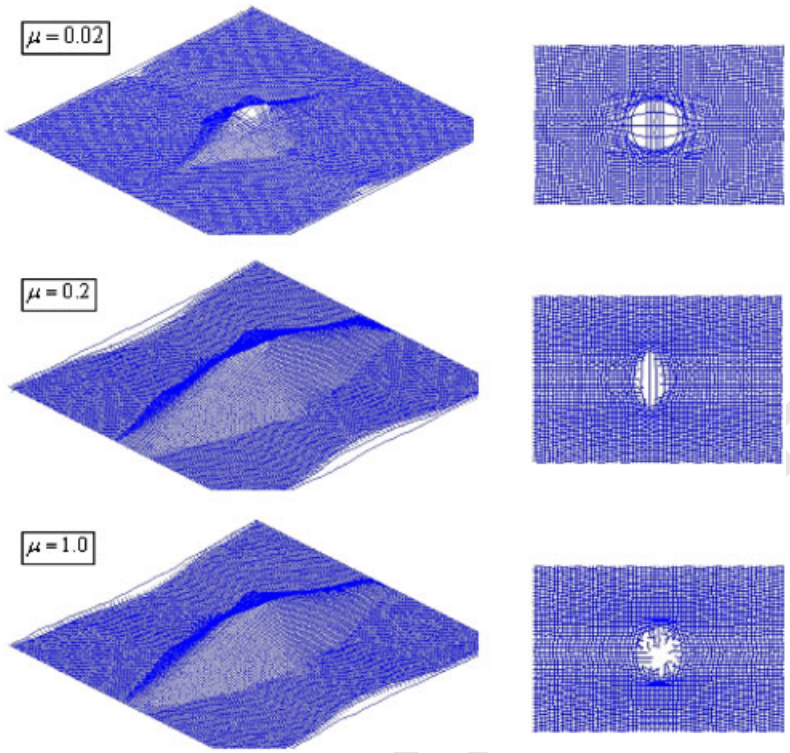

Color Online, B&W in Print

Figure 12. Simulation results for fabric perforation with different inter-yarn friction coefficients (impact velocity = 260 m/s).

of friction ($\mu = 0.06$–0.2), energy absorption by the fabric increases with impact velocity until about 250 m/s before it decreases with further increase in impact velocity. A friction coefficient of $\mu = 0.2$ yields the highest energy absorption for the whole range of impact velocities. At high friction coefficients greater than 0.2, the energy absorbed start to decrease when the friction coefficient is increased.

A better understanding of the effects of friction coefficient can be obtained by studying the fabric response at specific impact velocities for different friction coefficients. Figure 14 presents the variation of projectile velocity with time for an impact velocity of 260 m/s. The gradient is very gentle for low friction coefficients ($\mu = 0$–0.08). Primary yarns which are in direct contact with the projectile gradually slip aside during impact, leaving fewer and fewer primary yarns to retard the projectile. Hence, the fabric offers a very low projectile resistance. A friction coefficient of at least 0.1 is required to prevent yarns from slipping off the projectile and to maintain integrity of the weave at the impact point. The rate of decrease in projectile velocity is greatest for $\mu = 0.2$. In the case of $\mu = 1.0$, the projectile velocity history is similar to that for $\mu = 0.2$ except that perforation occurs earlier at 73 μs after impact. A high friction coefficient ($\mu = 1.0$) restrains relative slippage between yarns and causes stress concentration at the impact point, leading to a shorter time to failure.

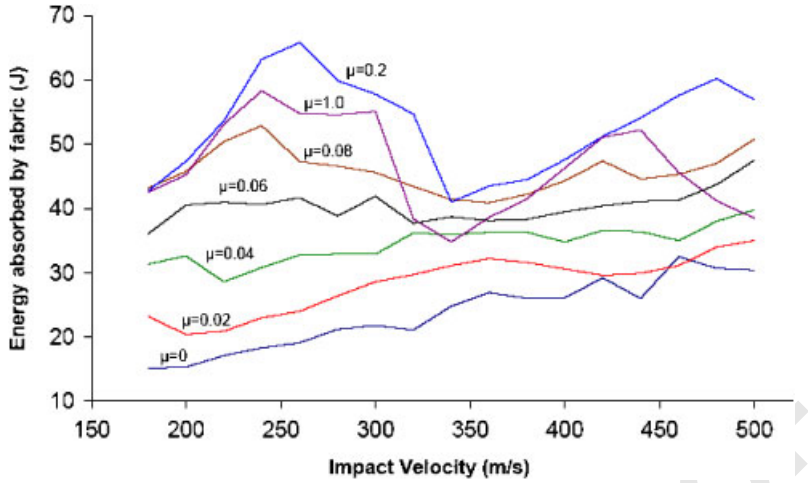

Color Online, B&W in Print

Figure 13. Variation of energy absorbed by fabric with impact velocity for different yarn friction coefficients.

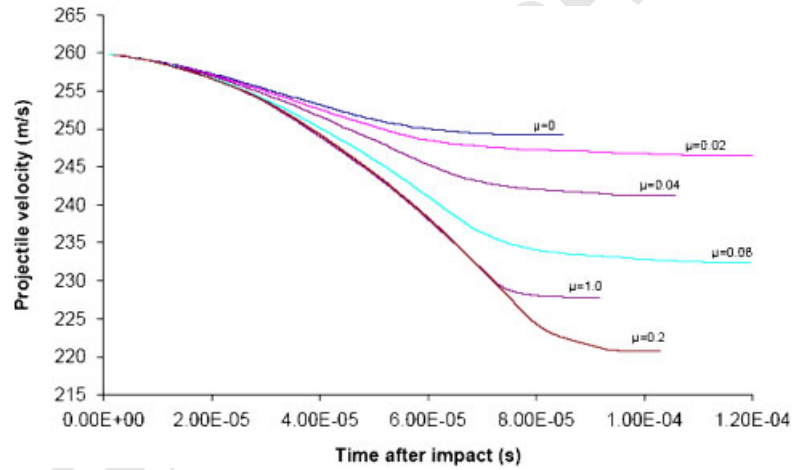

Color Online, B&W in Print

Figure 14. Projectile velocity histories for 260 m/s impact on fabric with different yarn friction coefficients.

The projectile impact energy is dissipated by the fabric via kinetic energy transferred to the fabric and strain energy in deformed yarns. The variation of these energy components for an impact velocity of 260 m/s is shown in Figure 15 for different friction coefficients. Both the kinetic energy and strain energy increase with the friction coefficient up to a value of $\mu = 0.2$. For higher values of inter-yarn friction, the energy trends appear similar up to the point of perforation, which occurs earlier for a higher friction coefficient. This is exemplified by the curves for $\mu = 0.2$ and $\mu = 1.0$. Although yarn friction clearly affects the amount energy

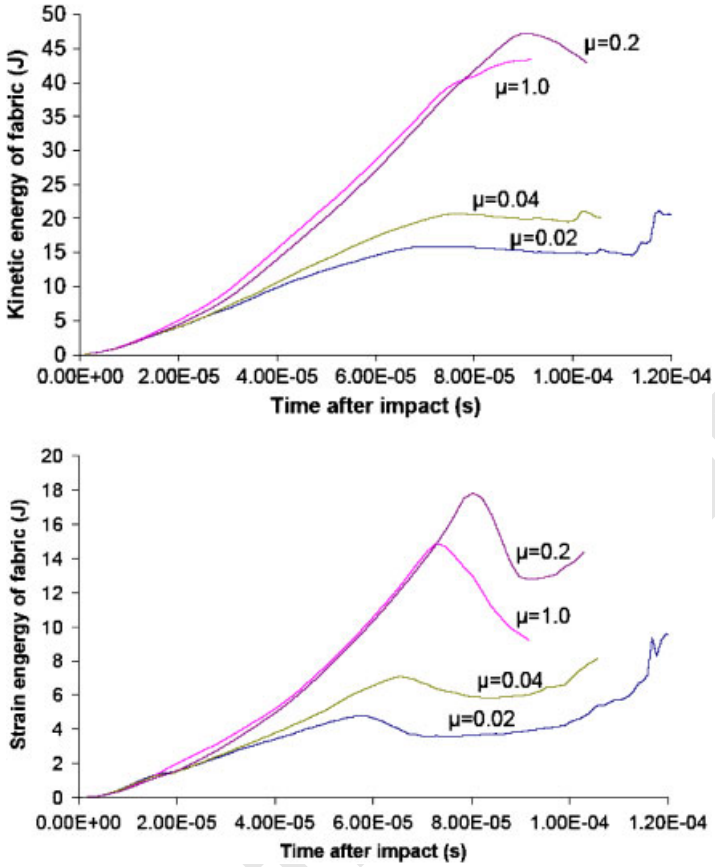

Color Online, B&W in Print

Figure 15. Kinetic energy and strain energy histories for impact at 260 m/s on fabric with different inter-yarn friction coefficients.

absorbed by the fabric, energy losses through friction are insignificant. For a friction coefficient of $\mu = 0.2$, frictional losses are only about 1 J.

8. EFFECTS OF INTER-YARN FRICTION ON THE FABRIC BALLISTIC LIMIT

The ballistic limit (BL) is another measure of the effectiveness of fabric armour in resisting ballistic impact. As shown in Figure 16, the BL increases with inter-yarn friction for values of μ from 0 to 0.1. The BL for $\mu = 0.1$ is almost twice that for perfectly smooth yarns ($\mu = 0$). The BL for $\mu = 0.2$ (70 m/s) is the same as the BL for $\mu = 0.1$ (71 m/s). Further increases in the friction coefficient, from a value of 0.2–0.6 yields little difference in the BL. As a reference, the BL obtained from a fabric model with pin-jointed crossover points that does not cater for sliding between yarns [8] is also plotted. This can be regarded as an extreme case

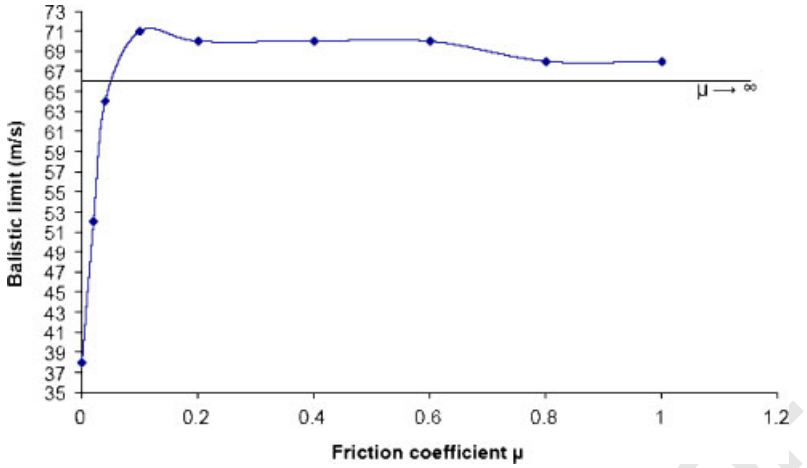

Color Online, B&W in Print

Figure 16. Variation of predicted ballistic limit with inter-yarn friction coefficient.

where the coefficient of friction is infinite ($\mu = \infty$). The results show that an excessively high friction coefficient has a negative effect on the BL.

Figure 17 shows predictions of fabric deformation at the BL for different inter-yarn friction coefficients. Perforation of the fabric for the case of $\mu = 0.02$ corresponds to extensive slippage of yarns over the projectile near the point of impact. No yarns are broken and yarn ravelling is obvious at the unclamped edges. The woven structure has poor integrity because of the low contact friction between yarns. A friction coefficient of $\mu = 0.1$ is required to preserve the structural coherence of fabric and for the crossover points of yarns to transmit energy effectively throughout the fabric. Hence, the BL is much higher than that for $\mu = 0.02$. Deformation and perforation of the fabric at the BL for $\mu = 0.2$ and $\mu = 1.0$ do not show much difference. The decrease in BL for higher friction coefficients of $\mu = 0.8$–1.0 arises from stress concentrations at the region of impact because of lack of mobility between yarns.

9. CONCLUSIONS

A numerical model for woven fabric armour, comprising a network of pin-jointed linear viscoelastic elements is developed and implemented through an in-house code. Accommodation of inter-yarn slippage is incorporated into the model to facilitate a more realistic representation of the woven architecture of fabrics. This is effected with minimal degrees of freedom and yet able to identify the effects of friction between yarns.

The viscoelastic parameters of the linear elements were obtained by fitting a Zener viscoelastic model to experimental data reported by Gu [22]. Comparisons of computational simulations with actual ballistic tests show that the proposed model yields good predictions of the fabric deformation and perforation mechanisms, as well as the fabric energy absorption characteristics.

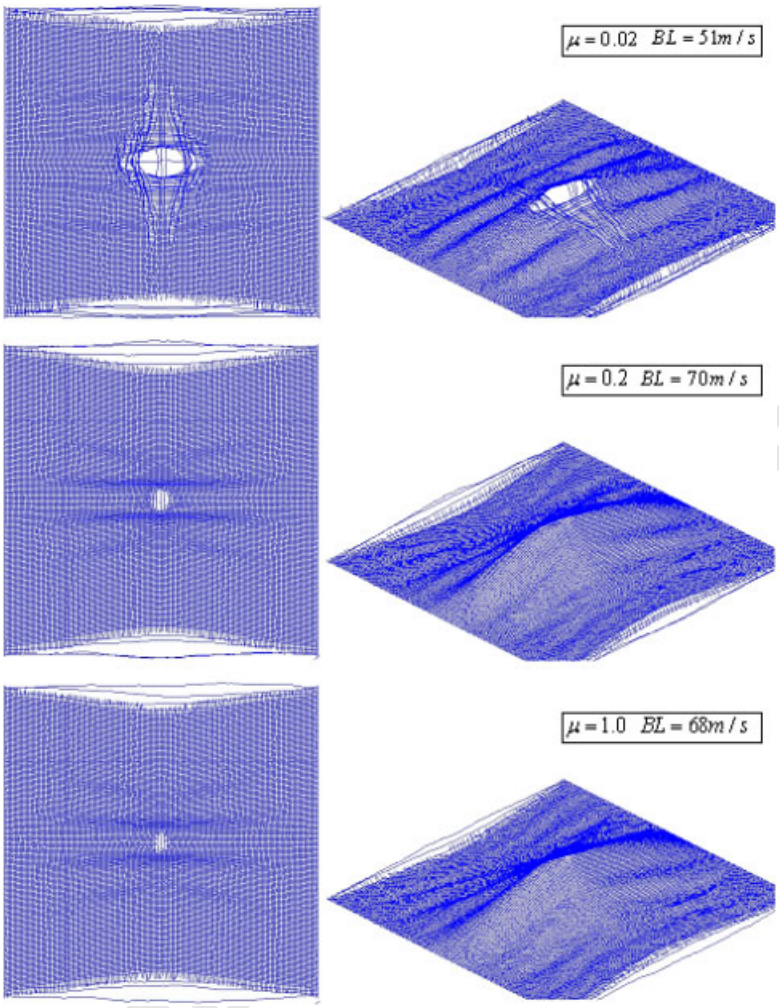

Color Online, B&W in Print

Figure 17. Simulation results for fabric with different inter-yarn friction coefficients perforated at the ballistic limit.

Simulations of ballistic impact on woven fabric with different values of inter-yarn friction show that the influence of friction on ballistic performance can be categorized into three levels of friction—low friction ($\mu = 0$–0.06), moderate friction ($\mu = 0.06$–0.2) and high friction ($\mu > 0.2$). Low friction coefficients lead to poor weave integrity and undermine the ability of the fabric to arrest projectiles. Excessive friction reduces relative sliding between yarns, resulting in high stress concentrations at the point of impact and give rise to premature yarn rupture. The ballistic resistance of a woven fabric appears to remain constant when the inter-yarn friction coefficient exceeds 0.2.

REFERENCES

1. Tan VBC, Tay TE, Teo WK. Strengthening fabric armour with silica colloidal suspensions. *International Journal of Solids and Structures* 2005; **42**:1561–1576.
2. Lee YS, Wetzel ED, Wagner NJ. The ballistic impact performance of Kevlar woven fabric impregnated with a colloidal shear thickening fluid. *Journal of Materials Science* 2003; **38**(13):2825–2833.
3. Tan VBC, Lim CT, Cheong CH. Perforation of high-strength fabric by projectiles of different geometry. *International Journal on Impact Engineering* 2003; **28**:207–222.
4. Lim CT, Tan VBC, Cheong CH. Perforation of high-strength double-ply fabric system by varying shaped projectiles. *International Journal on Impact Engineering* 2002; **27**:577–591.
5. Taylor Jr WJ, Vinson JR. Modeling ballistic impact into flexible materials. *AIAA Journal* 1990; **28**(12).
6. Lim CT, Shim VPW, Ng YH. Finite-element modeling of the ballistic impact of fabric armor. *International Journal of Impact Engineering* 2003; **28**:13–31.
7. Roylance D, Wang SS. Penetration mechanics of textile structures. In *Ballistic Materials and Penetration Mechanics*, Laible RC (ed.). Elsevier: Amsterdam, 1980.
8. Shim VPW, Tan VBC, Tay TE. Modeling deformation and damage characteristics of woven fabric under small projectile impact. *International Journal on Impact Engineering* 1995; **16**(4):585–605.
9. Johnson GR, Beissel SR, Cunniff PM. A computational model for fabric subjected to ballistic impact. *18th International Symposium Ballistics*, 1999.
10. Tabiei A, Ivanov I. Computational micro-mechanical model of flexible woven fabric for finite element impact simulation. *International Journal for Numerical and Mechanical Engineering* 2002; **53**:1259–1276.
11. Tabiei A, Ivanov I. Materially and geometrically non-linear woven composite micro-mechanical model with failure for finite element simulations. *International Journal of Non-Linear Mechanics* 2004; **39**(2):175–188.
12. Shockey DA, Erlich DC, Simons JW. Lightweight fragment barriers for commercial aircraft. *18th International Symposium on Ballistics*, U.S., 1999.
13. Duan Y, Keefe M, Bogetti TA, Cheeseman BA. Modeling the role of friction during ballistic impact of a high-strength plain-weave fabric. *Composite Structures* 2005; **68**(3):331–337.
14. Duan Y, Keefe M, Bogetti TA, Cheeseman BA. Modeling friction effects on the ballistic impact behavior of a single-ply high-strength fabric. *International Journal of Impact Engineering* 2005; **31**:996–1012.
15. Roylance D. Stress wave propagation in fibers: effect of crossovers. *Fiber Science and Technology* 1980; **13**:385–395.
16. Prosser RA. Penetration of nylon ballistic panels by fragment-simulating projectiles. Part 2: mechanism of penetration. *Textile Research Journal* 1988.
17. Bazhenov S. Dissipation of energy by bulletproof aramid fabric. *Journal of Material Science* 1997; **32**: 4167–4173.
18. Briscoe, BJ, Motamedi F. The ballistic impact characteristics of aramid fabrics: the influence of interface friction. *Wear* 1992; **158**(1–2):229–247.
19. Lee, BL, Walsh, TF, Won ST, Patts HM. Penetration failure mechanisms of armor-grade fiber composites under impact. *Journal of Composite Material* 2001; **35**(18):1605–1633.
20. Zavarise G, Wriggers P. Contact with friction between beams in 3-D space. *International Journal for Numerical Methods in Engineering* 2000; **49**:977–1006.
21. Johnson GR, Stryk RA. Symmetric contact and sliding interface algorithms for intense impulsive loading computations. *Computer Methods in Applied Mechanics and Engineering* 2001; **190**:4531–4549.
22. Gu B. Analytical modeling for the ballistic perforation of planar plain-woven fabric target by projectile. *Composites*: *Part B* 2003; **34**:361–371.
23. Rebouillat S. Tribological properties of woven para-aramid fabrics and their constituent yarns. *Journal on Material Science* 1998; **33**:3293–3301.

John Wiley & Sons Ltd
The Atrium, Southern Gate, Chichester West, Sussex PO19 8S

Author Queries For NME 1596

While preparing this paper/manuscript for typesetting, the following queries have arisen

Query No	Proof Page / line no	Details required	Authors Response
1	9/3	Please check 'It should be noted that the friction force f_t applied to ...' is okay (aftr Eq. (14)).	
2	REF	Please provide page range for ref[5].	
3	REF	Please check the journal expansion for ref[10],[15] is ok.	

COPYRIGHT TRANSFER AGREEMENT

Wiley Production No. .....

Re: Manuscript entitled .....

(the "Contribution") written by .....

(the "Contributor") for publication in.....

(the "Journal) published by John Wiley & Sons Ltd ("Wiley").

In order to expedite the publishing process and enable Wiley to disseminate your work to the fullest extent, we need to have this Copyright Transfer Agreement signed and returned to us with the submission of your manuscript. If the Contribution is not accepted for publication this Agreement shall be null and void.

A. COPYRIGHT

1. The Contributor assigns to Wiley, during the full term of copyright and any extensions or renewals of that term, all copyright in and to the Contribution, including but not limited to the right to publish, republish, transmit, sell, distribute and otherwise use the Contribution and the material contained therein in electronic and print editions of the Journal and in derivative works throughout the world, in all languages and in all media of expression now known or later developed, and to license or permit others to do so.
2. Reproduction, posting, transmission or other distribution or use of the Contribution or any material contained therein, in any medium as permitted hereunder, requires a citation to the Journal and an appropriate credit to Wiley as Publisher, suitable in form and content as follows: (Title of Article, Author, Journal Title and Volume/Issue Copyright © [year] John Wiley & Sons Ltd or copyright owner as specified in the Journal.)

B. RETAINED RIGHTS

Notwithstanding the above, the Contributor or, if applicable, the Contributor's Employer, retains all proprietary rights other than copyright, such as patent rights, in any process, procedure or article of manufacture described in the Contribution, and the right to make oral presentations of material from the Contribution.

C. OTHER RIGHTS OF CONTRIBUTOR

Wiley grants back to the Contributor the following:

1. The right to share with colleagues print or electronic "preprints" of the unpublished Contribution, in form and content as accepted by Wiley for publication in the Journal. Such preprints may be posted as electronic files on the Contributor's own website for personal or professional use, or on the Contributor's internal university or corporate networks/intranet, or secure external website at the Contributor's institution, but not for commercial sale or for any systematic external distribution by a third party (eg: a listserver or database connected to a public access server). Prior to publication, the Contributor must include the following notice on the preprint: "This is a preprint of an article accepted for publication in [Journal title] Copyright © (year) (copyright owner as specified in the Journal)". After publication of the Contribution by Wiley, the preprint notice should be amended to read as follows: "This is a preprint of an article published in [include the complete citation information for the final version of the Contribution as published in the print edition of the Journal]" and should provide an electronic link to the Journal's WWW site, located at the following Wiley URL: http://www.interscience.wiley.com/. The Contributor agrees not to update the preprint or replace it with the published version of the Contribution.
2. The right, without charge, to photocopy or to transmit on-line or to download, print out and distribute to a colleague a copy of the published Contribution in whole or in part, for the Contributor's personal or professional use, for the advancement of scholarly or scientific research or study, or for corporate informational purposes in accordance with paragraph D2 below.
3. The right to republish, without charge, in print format, all or part of the material from the published Contribution in a book written or edited by the Contributor.
4. The right to use selected figures and tables, and selected text (up to 250 words) from the Contribution, for the Contributor's own teaching purposes, or for incorporation within another work by the Contributor that is made part of an edited work published (in print or electronic format) by a third party, or for presentation in electronic format on an internal computer network or external website of the Contributor or the Contributor's employer. The abstract shall not be included as part of such selected text.
5. The right to include the Contribution in a compilation for classroom use (course packs) to be distributed to students at the Contributor's institution free of charge or to be stored in electronic format in datarooms for access by students at the Contributor's institution as part of their course work (sometimes called "electronic reserve rooms") and for in-house training programmes at the Contributor's employer.

D. CONTRIBUTIONS OWNED BY EMPLOYER

1. If the Contribution was written by the Contributor in the course of the Contributor's employment (as a "work-made-for-hire" in the course of employment), the Contribution is owned by the company/employer which must sign this Agreement (in addition to the Contributor's signature), in the space provided below. In such case, the company/employer hereby assigns to Wiley, during the full term of copyright, all copyright in and to the Contribution for the full term of copyright throughout the world as specified in paragraph A above.
2. In addition to the rights specified as retained in paragraph B above and the rights granted back to the Contributor pursuant to paragraph C above, Wiley hereby grants back, without charge, to such company/employer, its subsidiaries and divisions, the right to make copies of and distribute the published Contribution internally in print format or electronically on the Company's internal network. Upon payment of the Publisher's reprint fee, the institution may distribute (but not re-sell) print copies of the published Contribution externally. Although copies so made shall not be available for individual re-sale, they may be included by the company/employer as part of an information package included with software or other products offered for sale or license. Posting of the published Contribution by the institution on a public access website may only be done with Wiley's written permission, and payment of any applicable fee(s).

E. GOVERNMENT CONTRACTS

In the case of a Contribution prepared under US Government contract or grant, the US Government may reproduce, without charge, all or portions of the Contribution and may authorise others to do so, for official US Government purposes only, if the US Government contract or grant so requires. (Government Employees: see note at end.)

F. COPYRIGHT NOTICE

The Contributor and the company/employer agree that any and all copies of the Contribution or any part thereof distributed or posted by them in print or electronic format as permitted herein will include the notice of copyright as stipulated in the Journal and a full citation to the Journal as published by Wiley.

G. CONTRIBUTOR'S REPRESENTATIONS

The Contributor represents that the Contribution is the Contributor's original work. If the Contribution was prepared jointly, the Contributor agrees to inform the co-Contributors of the terms of this Agreement and to obtain their signature(s) to this Agreement or their written permission to sign on their behalf. The Contribution is submitted only to this Journal and has not been published before, except for "preprints" as permitted above. (If excerpts from copyrighted works owned by third parties are included, the Contributor will obtain written permission from the copyright owners for all uses as set forth in Wiley's permissions form or in the Journal's Instructions for Contributors, and show credit to the sources in the Contribution.) The Contributor also warrants that the Contribution contains no libelous or unlawful statements, does not infringe on the right or privacy of others, or contain material or instructions that might cause harm or injury.

Tick one box and fill in the appropriate section before returning the original signed copy to the Publisher

☐ ***Contributor-owned work***

Contributor's signature ..... Date .....

Type or print name and title .....

Co-contributor's signature ..... Date .....

Type or print name and title .....

Attach additional signature page as necessary

☐ ***Company/Institution-owned work (made-for-hire in the course of employment)***

Contributor's signature ..... Date .....

Type or print name and title .....

Company or Institution
(Employer-for Hire) .....

Authorised signature of Employer ..... Date .....

Type or print name and title .....

☐ ***US Government work***

Note to US Government Employees

A Contribution prepared by a US federal government employee as part of the employee's official duties, or which is an official US Government publication is called a "US Government work", and is in the public domain in the United States. In such case, the employee may cross out paragraph A1 but must sign and return this Agreement. If the Contribution was not prepared as part of the employee's duties or is not an official US Government publication, it is not a US Government work.

☐ ***UK Government work (Crown Copyright)***

Note to UK Government Employees

The rights in a Contribution by an employee of a UK Government department, agency or other Crown body as part of his/her official duties, or which is an official government publication, belong to the Crown. In such case, the Publisher will forward the relevant form to the Employee for signature.

WILEY AUTHOR DISCOUNT CARD

As a highly valued contributor to Wiley's publications, we would like to show our appreciation to you by offering a **unique 25% discount** off the published price of any of our books*.

To take advantage of this offer, all you need to do is apply for the **Wiley Author Discount Card** by completing the attached form and returning it to us at the following address:

The Database Group
John Wiley & Sons Ltd
The Atrium
Southern Gate
Chichester
West Sussex PO19 8SQ
UK

In the meantime, whenever you order books direct from us, simply quote promotional code **S001W** to take advantage of the 25% discount.

The newest and quickest way to order your books from us is via our new European website at:

http://www.wileyeurope.com

Key benefits to using the site and ordering online include:

- Real-time SECURE on-line ordering
- The most up-to-date search functionality to make browsing the catalogue easier
- Dedicated Author resource centre
- E-mail a friend
- Easy to use navigation
- Regular special offers
- Sign up for subject orientated e-mail alerts

So take advantage of this great offer, return your completed form today to receive your discount card.

Yours sincerely,

Verity Leaver
E-marketing and Database Manager

*TERMS AND CONDITIONS

This offer is exclusive to Wiley Authors, Editors, Contributors and Editorial Board Members in acquiring books (excluding encyclopaedias and major reference works) for their personal use. There must be no resale through any channel. The offer is subject to stock availability and cannot be applied retrospectively. This entitlement cannot be used in conjunction with any other special offer. Wiley reserves the right to amend the terms of the offer at any time.

REGISTRATION FORM
FOR 25% BOOK DISCOUNT CARD

To enjoy your special discount, tell us your areas of interest and you will receive relevant catalogues or leaflets from which to select your books. Please indicate your specific subject areas below.

Accounting [ ]
- Public [ ]
- Corporate [ ]

Chemistry [ ]
- Analytical [ ]
- Industrial/Safety [ ]
- Organic [ ]
- Inorganic [ ]
- Polymer [ ]
- Spectroscopy [ ]

Encyclopedia/Reference [ ]
- Business/Finance [ ]
- Life Sciences [ ]
- Medical Sciences [ ]
- Physical Sciences [ ]
- Technology [ ]

Earth & Environmental Science [ ]

Hospitality [ ]

Genetics [ ]
- Bioinformatics/Computational [ ]
  Biology [ ]
- Proteomics [ ]
- Genomics [ ]
- Gene Mapping [ ]
- Clinical Genetics [ ]

Medical Science [ ]
- Cardiovascular [ ]
- Diabetes [ ]
- Endocrinology [ ]
- Imaging [ ]
- Obstetrics/Gynaecology [ ]
- Oncology [ ]
- Pharmacology [ ]
- Psychiatry [ ]

Non-Profit [ ]

Architecture [ ]

Business/Management [ ]

Computer Science [ ]
- Database/Data Warehouse [ ]
- Internet Business [ ]
- Networking [ ]
- Programming/Software [ ]
  Development [ ]
- Object Technology [ ]

Engineering [ ]
- Civil [ ]
- Communications Technology [ ]
- Electronic [ ]
- Environmental [ ]
- Industrial [ ]
- Mechanical [ ]

Finance/Investing [ ]
- Economics [ ]
- Institutional [ ]
- Personal Finance [ ]

Life Science [ ]

Landscape Architecture [ ]

Mathematics/Statistics [ ]

Manufacturing [ ]

Material Science [ ]

Psychology [ ]
- Clinical [ ]
- Forensic [ ]
- Social & Personality [ ]
- Health & Sport [ ]
- Cognitive [ ]
- Organizational [ ]
- Developmental and Special Ed [ ]
- Child Welfare [ ]
- Self-Help [ ]

Physics/Physical Science [ ]

[ ] I confirm that I am a Wiley Author/Editor/Contributor/Editorial Board Member of the following publications:

SIGNATURE: .....

PLEASE COMPLETE THE FOLLOWING DETAILS IN BLOCK CAPITALS:

TITLE AND NAME: (e.g. Mr, Mrs, Dr) .....

JOB TITLE: .....

DEPARTMENT: .....

COMPANY/INSTITUTION: .....

ADDRESS: .....

.....

.....

.....

TOWN/CITY: .....

COUNTY/STATE: .....

COUNTRY: .....

POSTCODE/ZIP CODE: .....

DAYTIME TEL: .....

FAX: .....

E-MAIL: .....

YOUR PERSONAL DATA
We, John Wiley & Sons Ltd, will use the information you have provided to fulfil your request. In addition, we would like to:

1. Use your information to keep you informed by post, e-mail or telephone of titles and offers of interest to you and available from us or other Wiley Group companies worldwide, and may supply your details to members of the Wiley Group for this purpose.

   [ ] Please tick the box if you do not wish to receive this information

2. Share your information with other carefully selected companies so that they may contact you by post, fax or e-mail with details of titles and offers that may be of interest to you.

   [ ] Please tick the box if you do not wish to receive this information.

If, at any time, you wish to stop receiving information, please contact the Database Group (databasegroup@wiley.co.uk) at John Wiley & Sons Ltd, The Atrium, Southern Gate, Chichester, West Sussex PO19 8SQ, UK.

E-MAIL ALERTING SERVICE
We offer an information service on our product ranges via e-mail. If you do not wish to receive information and offers from John Wiley companies worldwide via e-mail, please tick the box [ ].

This offer is exclusive to Wiley Authors, Editors, Contributors and Editorial Board Members in acquiring books (excluding encyclopaedias and major reference works) for their personal use. There should be no resale through any channel. The offer is subject to stock availability and may not be applied retrospectively. This entitlement cannot be used in conjunction with any other special offer. Wiley reserves the right to vary the terms of the offer at any time.

Ref: S001W